Innovative Infrastructure Solutions (2023) 8:63
https://doi.org/10.1007/s41062-022-01028-y

TECHNICAL PAPER

Multiscale soft computing-based model of shear strength of steel fibre-reinforced concrete beams

Saif Alzabeebee[1] · Rwayda Kh. S. Al-Hamd[2] · Ali Nassr[3] · Mohammed Kareem[4,5] · Suraparb Keawsawasvong[6]

Received: 16 August 2022 / Accepted: 26 December 2022
© The Author(s) 2023

Abstract

Concrete is weak in tension, so steel fibres are added to the concrete members to increase shear capability. The shear capacity of steel fibre-reinforced concrete (SFRC) beams is crucial when building reinforced concrete structures. Creating a precise equation to determine the shear resistance of SFRC beams is challenging since many factors can influence the shear capacity of these beams. In addition, the precision available equations to predict the shear capacity are examined. The current research aims to examine the available equations and propose novel and more accurate model to predict the shear capacity of SFRC beams. An innovative evolutionary polynomial regression analysis (EPR- MOGA) is utilized to propose the new equation. The proposed equation offered improved prediction and increased accuracy compared to available equations, where it scored a lower mean absolute error (MAE) and root mean square error (RMSE), a mean (μ) close to the optimum value of 1.0 and a higher coefficient of determination (R^2) when a comparison with literature was conducted. Therefore, the new equation can be employed to assure more resilient and optimized design calculations due to their improved performance.

Keywords EPR-MOGA · Statistical analysis · SFRC beams · Shear capacity · Concrete beams

✉ Rwayda Kh. S. Al-Hamd
r.al-hamd@abertay.ac.uk

Saif Alzabeebee
Saif.Alzabeebee@qu.edu.iq

Ali Nassr
adnn201@exeter.ac.uk

Mohammed Kareem
mohammedkareem999@gmail.com

Suraparb Keawsawasvong
ksurapar@engr.tu.ac.th

1 Department of Roads and Transport Engineering, University of Al-Qadisiyah, Al-Qadisiyah, Iraq

2 School of Applied Sciences, Abertay University, Dundee DD1 1HG, Scotland, UK

3 Department of Civil Engineering, College of Engineering, University of Anbar, Ramadi, Anbar, Iraq

4 Institute of Concrete Structures, Technical University Dresden, Dresden, Germany

5 Department of Civil Engineering, University of Al-Qadisiyah, Al-Qadisiyah, Iraq

6 Department of Civil Engineering, Thammasat School of Engineering, Thammasat University, Khlong Luang District 12120, Pathumthani, Thailand

Introduction

Concrete has always been considered a brittle material that cannot withstand tensile or shear pressures. When exposed to external loads, reinforced concrete beams are susceptible to high shear stresses. Any reinforced concrete (RC) member that cracks experiences a different state of stress than the theory of linear elasticity predicts because the region between the flexural tension and flexural compression zones is compromised. Consequently, it becomes crucial to consider how shear transmits in a cracked RC member. It is challenging to comprehend the relative contribution of the transmission mechanisms to the shear capacity because of the complicated interactions of shear stresses [6, 7]. The following shear transfer methods can be found in the ASCE-ACI Committee 445 report [2]:

- Shear strains in the uncracked section's flexural compression zone.
- Crack friction, interface shear transmission, or aggregate interlock.
- Dowel's action.
- The transient tensile stress transfer.

Published online: 07 January 2023

Practitioners' primary concern is preventing these tensile and shear failures. Thus, various methods have been introduced to enhance shear resistance, including steel fibres, which have been improved in the last decade. Tests on the concrete fibre material in both structural and non-structural applications have shown it to be reliable. Ground- and pile-supported slabs, tunnel linings, different precast components, raft foundations, industrial pavement, and intricate architectural forms are some examples of steel fibre-reinforced concrete's practical applications [19].

Researchers have explored the parameters that impact the shear since the early 1970s. Batson et al. [18] conducted a study that looked at the influence of the volume percentage of steel fibres (*Vf* and the shear span to depth ratio (a/d; and found that adding steel fibres substantially increases the shear strength of members. Further research by Swamy and Bahia [36, 37] demonstrated that the shear strength of steel fibre reinforced concrete (SFRC rectangular and T-shaped beams was much higher than that of the reinforced concrete beams without shear reinforcement. The shear performance of SFRC members was examined by Mansur et al. [29], Lim et al. [28], and Narayanan and Darwish [30]. By utilizing test factors such as concrete compressive strength (*fc*), the volume fraction of steel fibres (*Vf*), shear span/effective depth ratio (a/d), and longitudinal steel ratio (ρ), they sought to explain the complex shear process of SFRC beams. Shear experiments on SFRC beams were undertaken by Narayanan and Darwish [30] and focused on the impact of tensile strength. They suggested a shear strength equation based on the shear contributions of steel fibre and concrete under the assumption of a 45 °crack angle, with a fibre factor (F) incorporated to account for the effect of geometry and volume percentage of fibre on the SFRC member's shear capacity.

By revising the shear strength equations of ACI 318 [1] and Zsutty [40], Ashour et al. [17] created two equations for determining the shear strength of steel fibre reinforced high-strength concrete (SFRHC) beams based on shear testing of SFRHC beams (1968). In addition, Kwak et al. [27], Oh and Kim [32], and Karl et al. [24] proposed shear strength estimation equation based on the acquired experimental data for SFRC and SFRHC beams. In 2021, Sharifi and Moghbeli [35] and Tarawneh et al. [39] used the artificial neural network (ANN) approach to refine the shear prediction presented in the literature and they were able to get a better prediction compared to previous studies.

Based on this review, it is evident that there is a need to examine the accuracy of the available equations of the shear strength of steel fibre-reinforced concrete beams. In addition, it is also clear that there are limited attempts to implicate soft computing approaches to develop robust models to predict the shear capacity of SFRC beams, where only the ANN is utilized. However, evidence in the literature showed that soft computing approaches could provide better predictions compared to the ANN [3, 4, 8, 22, 34]. Thus, this study uses a novel approach that combines regression analysis with the AI (EPR-MOGA) to develop new correlation to predict the shear strength of steel fibre-reinforced concrete beams. In addition, this study also assesses the accuracy of the available equations developed to predict the shear capacity of SFRC beams.

Available equations to predict the shear strength of steel fibre reinforced concrete beams

A survey of the literature was carried out to collect and understand the available predictive equations of the shear strength of steel fibre-reinforced concrete beams (Swamy and Al-Taan, [38]; [29, 30], Al-Ta'an and Al-Fee, [5]; [17, 20, 23, 25–27, 35, 39]. The result of this literature survey was 12 predictive equations. These equations are listed in Table 1. These equations will be assessed as part of this research to check their accuracy and see if these equations could be used with confidence in practice. The assessment will also show the performance of the model developed in this research.

ρ: is the flexural reinforcement ratio, $f_c^{'}$: is the cylinder compressive strength, $f_{\mathrm{cu}}^{'}$: is the cube compressive strength, and it can be taken as $0.8f_c^{'}$, τ: is the average fibre matrix interfacial bond stress, a: is the shear span, d: is the effective depth, λ: is the arch action factor, and it is equal to 1.0 for $a/d > 2.8$, and $2.8d/a$ for$a/d \le 2.8$, F: is the fibre factor, and it is equal to $(l_f/d_f)V_f$, l_f: is the fibre length, d_f: is the fibre diameter, V_f: is the volume fraction of steel fibres, Ω: is the arch action factor and it is equal to 1.0 for $a/d > 3.4$, and $3.4d/a$ for$a/d \le 3.4$, e: is the arch action factor and it is equal to 1.0 for, $a/d > 2.5$, and $2.5d/a$ for$a/d \le 2.5$, V: is the shear force, M: is the bending moment, α: is the arch action factor and it is equal to 1.0 for $a/d \ge 2.5$, and $2.5d/a \le 3$ for$a/d < 2.5$, A_u: is a factor and it is given as 0.65, B_u: is a factor and it is given as $B_u = 0.01162\frac{l_f}{d_f} - 0.214$, C_u: is a factor and it is given as $C_u = -0.00552\frac{l_f}{d_f} + 0.24$, D_u: is a factor and it is given as $D_u = 0.00045\frac{l_f}{d_f} - 0.026$, and$d$: is the effective depth.

Methodology

Data collection

As a result, database has been compiled from the study of Sharifi and Moghbeli [35], who developed this database

Table 1 Predictive equations available in the literature of the shear strength of SFRHC beams

Reference	Equation
Al-Ta'an and Al-Fee [5]	$v_{\mathrm{frc}} = e\left(0.17\sqrt{f_c'} + 106\rho\frac{d}{a}\right) + 1.128F$
Ashour et al. [17]	$v_{\mathrm{frc}} = \left(0.7\sqrt{f_c'} + 7F\right)\frac{d}{a} + 17.2\rho\frac{d}{a}$
Gandomi et al. [20]	$v_{\mathrm{frc}} = \frac{2d}{a}\left(\rho f_c' + 0.41\tau F\right) + \frac{d}{2a}\frac{\rho}{(288\rho-11)^4} + 2$
Kara [23]	$v_{\mathrm{frc}} = \left(\frac{\rho}{3.022\left(\frac{a}{d}\right)}\right)^3 + \frac{Fd^{\frac{1}{4}}}{2.289} + \sqrt{\frac{9.436f_c'}{d}}$
Khaloo and Kim [25]	$v_{\mathrm{frc}} = \left(A_u + B_u V_f + C_u V_f^2 + D_u V_f^3\right)\sqrt{f_c'}$
Khuntia et al. [26]	$v_{frc} = (0.167\alpha + 0.25F)\sqrt{f_c'}$
Kwak et al. [27]	$v_{\mathrm{frc}} = 3.7\left(\Omega\left(\frac{f_{cu}'}{20-\sqrt{F}} + 0.7 + \sqrt{F}\right)^{\frac{2}{3}}\left(\rho\frac{d}{a}\right)^{\frac{1}{3}}\right) + 0.328\tau F$
Mansur et al. [29]	$v_{\mathrm{frc}} = \left(0.16\sqrt{f_c'} + 17.2\rho\frac{Vd}{M}\right) + 0.41\tau V_f\frac{l_f}{d_f}$
Narayanan and Darwish [30]	$v_{\mathrm{frc}} = \lambda\left(0.24\left(\frac{f_{cu}'}{20-\sqrt{F}} + 0.7 + \sqrt{F}\right) + 80\left(\rho\frac{d}{a}\right)\right) + 0.41\tau F$
Swamy and Al-Taan [29]	$v_{\mathrm{frc}} = 0.167\sqrt{f_c'} + 0.37\tau V_f\frac{l_f}{d_f}$
Sharifi and Moghbeli [35]	$v_{\mathrm{frc}} = (6.261 + \frac{21.812}{1+e^{-\beta_1}} - \frac{25.275}{1+e^{-\beta_2}}$
Tarawneh et al. [39]	$v_{\mathrm{frc}} = \left(\left(\frac{-4.83}{\rho}\right)(f_c' - \rho)\right)^{\frac{1}{5}}\left(\rho + \frac{F}{\rho}\right)^{\frac{1}{4}}\left(\frac{(F(-2.18))-\rho}{F+\frac{a}{d}}\right)$

using the results of experimental studies available in the literature. In total, 235 test results (i.e., data points) have been collected and used. The collected data are the fibre content by volume (vf), the length of the fibre (lf), the diameter of the fibre (df), the ratio of the reinforcement in the longitudinal direction ($\rho 1$), the effective depth of the beam (d), the shear span (a), the compressive strength of the concrete (f_c'), and the shear capacity of the beam (v_{frc}).

A basic statistical analysis is carried out to find the basic statistical indicators of the collected database: the maximum value, minimum value, standard deviation, mean, and range. Table 2 presents the obtained results from this analysis.

EPR-MOGA

Evolutionary polynomial regression analysis (EPR-MOGA) is used to aid the development of the new model. EPR-MOGA stands for multi-objective evolutionary polynomial regression analysis, an intelligent computational method that leverages input data to generate a novel solution to a specific problem [10, 14]. This method is based on regression analysis and employs a genetic algorithm (GA) to create a mathematical model that can explain the relationship between physical input variables [21, 31]. The EPR-MOGA uses GA to find the best model automatically. This GA is further refined by the addition of several objectives to control model complexity and ensure the new model's accuracy and fitness [10, 21]. As a result, one of the key features of this regression method over traditional regression is that the searched algorithm automatically finds the optimal mathematical model. The EPR-MOGA does this by selecting candidate exponents and examining the accuracy of the developed correlation using a coefficient called the coefficient of determination (CD) (shown in Eq. 1). Then,

Table 2 Basic statistical indicators of the collected database

Indicator	vf	lf/df	$\rho 1$	d(mm)	a/d	f_c'(MPa)	v_{frc}(MPa)
Minimum value	0.002	19.000	0.010	76.000	0.460	20.600	0.770
Maximum value	0.075	133.000	0.057	766.500	5.000	111.500	19.190
Standard deviation	0.012	25.345	0.011	141.096	1.051	17.532	2.906
Mean	0.009	74.426	0.025	225.457	2.993	44.947	3.963
Range	0.073	114.000	0.047	690.500	4.540	90.900	18.420

the EPR-MOGA identifies, by several trails, the exponents arrangement that achieve the best accuracy. Also, in contrast to regression analysis, where the user must manually try every conceivable association, the user must provide the model structure, the number of model terms, and the range and step of the exponents. Also, the EPR-MOGA tackles the overfitting problem associated with conventional regression analysis methods that do not use AI. Further details on this method could be found in other publications (e.g., [9, 10, 12, 13, 41]. Figure 1 shows a flow chart of the EPR-MOGA analysis, which illustrates how the EPR-MOGA analysis works.

$$CD = 1 - \frac{\sum_n (Y_a - Y)^2}{\sum_n (Y_a - \frac{1}{n}\sum_n Y_p)^2} \quad (1)$$

where, Y_a is the dependent input value (i.e., the measured shear strength); Y is the predicted dependent input value from the EPR-MOGA correlation (i.e., the predicted shear strength); and n is the number of data points.

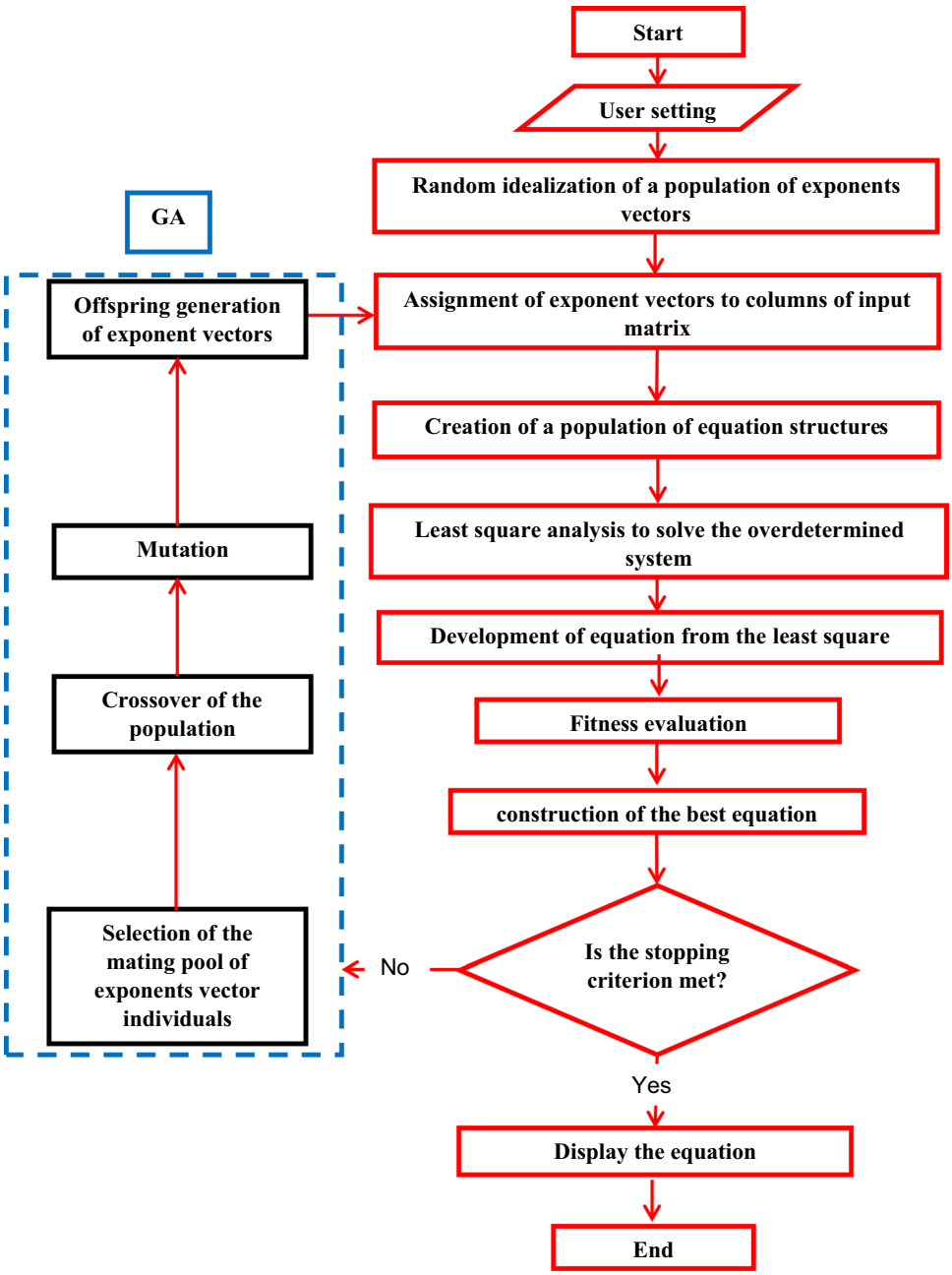

Fig. 1 Simple flow chart of the steps of the EPR-MOGA analysis [10, 15]

Statistical assessment

The performance of the existed equations and the proposed model are checked by calculating the mean absolute error (MAE), root mean square error (RMSE), mean (μ), and coefficient of determination (R^2). These accuracy checks are calculated with the aid of excel and using Eqs. 2–5 [42–44].

The overall error is checked by assessing the values of the MAE and RMSE. In addition, the overall over-and-under estimation is examined using the value of the mean, where a value higher than 1 indicates an overall over-estimation of the shear capacity and a value lower than 1 means an overall under-estimation in the prediction. Furthermore, the overall accuracy of the prediction is examined using the value of the R^2.

In addition to the accuracy checks, an error analysis is also carried out to investigate the cumulative frequency of the error to provide insight into the existing equations' performance and the new model.

$$\mathrm{MAE} = \frac{1}{n}\sum_{1}^{n}\left|v_{\mathrm{frc}(p)} - v_{\mathrm{frc}(m)}\right| \tag{2}$$

$$\mathrm{RMSE} = \sqrt{\frac{1}{n}\sum_{1}^{n}\left(v_{\mathrm{frc}(p)} - v_{\mathrm{frc}(m)}\right)^2} \tag{3}$$

$$\mu = \frac{1}{n}\sum_{1}^{n}\left(\frac{v_{\mathrm{frc}(p)}}{v_{\mathrm{frc}(m)}}\right) \tag{4}$$

$$R^2 = \left(\frac{\sum_{i=1}^{n}(v_{\mathrm{frc}(p)} - v_{\mathrm{frc}(p)_{\mathrm{average}}})(v_{\mathrm{frc}(m)} - v_{\mathrm{frc}(m)_{\mathrm{average}}})}{\sqrt{\sum_{i=1}^{n}(v_{\mathrm{frc}(p)} - v_{\mathrm{frc}(p)_{\mathrm{average}}})^2 \sum_{i=1}^{n}(v_{\mathrm{frc}(m)} - v_{\mathrm{frc}(m)_{\mathrm{average}}})^2}}\right)^2 \tag{5}$$

where, n is the number of inputs involved in the calculations, $v_{\mathrm{frc}(p)}$ is the predicted shear capacity of the SFRC beam, and $v_{\mathrm{frc}(m)}$ is the measured shear capacity of the SFRC beam.

Results

The presentation of the new model, the assessment of the existed equations, and the error analysis of the new model and the existed equations are discussed in this section as follows:

EPR-MOGA new model

The database discussed in "Data collection" Section is utilized to develop the new predictive model of the shear capacity of SFRC beams. This database is divided into two group: training group and testing group. 80% of the data are used as training data and the remaining data are considered a testing data. The training group is utilized to train the EPR-MOGA model, and the testing group is employed to assess the model's accuracy in predicting unseen scenarios that were not used in its development (i.e., training). The data separation into training and testing is conducted carefully to ensure that the maximum, minimum, and range of the testing data group are within the same range of that of the training data group to avoid extrapolations in the predictions of the model in the testing stage [11, 16]. After completing the dividing stage, this has been ensured by conducting a statistical analysis on both data groups. Tables 3 and 4 present the basic statistical indicators of the two group to demonstrate that the range of the testing data group employed in this study was within that of the training data.

The development of the model is carried out after dividing the data, where the two data groups are provided into

Table 3 Basic statistical indicators of the collected database

Indicator	vf	lf/df	$\rho 1$	d(mm)	a/d	f_c'(MPa)	v_{frc}(MPa)
Minimum value	0.002	19.000	0.010	76.000	0.460	20.600	1.000
Maximum value	0.075	133.000	0.057	766.500	5.000	111.500	19.190
Standard deviation	0.013	25.506	0.011	145.416	1.061	17.936	2.844
Mean	0.010	75.202	0.025	233.043	2.984	45.049	3.947
Range	0.073	114.000	0.047	690.500	4.540	90.900	18.190

Table 4 Basic statistical indicators of the collected database

Indicator	vf	lf/df	$\rho 1$	d(mm)	a/d	f_c'(MPa)	v_{frc}(MPa)
Minimum value	0.002	43.000	0.010	76.000	0.700	28.700	0.770
Maximum value	0.075	133.000	0.057	610.000	4.800	99.000	19.120
Standard deviation	0.011	24.713	0.011	118.884	1.021	15.991	3.172
Mean	0.009	71.319	0.024	195.117	3.027	44.538	4.029
Range	0.073	90.000	0.047	534.000	4.100	70.300	18.350

the algorithm of the EPR-MOGA to search for the best fit model and to test (validate) it. Many trials were carried out in this stage to examine the influence of the model's number of terms and exponents range on its prediction accuracy. As a result, the best model obtained from the EPR-MOGA is shown in Eq. 6. The statistical accuracy measures of the new model (i.e., MAE, RMSE, μ, and R^2) are presented in Table 5 for both data groups. In addition, Fig. 2a, b present the comparison of the predictions of the model in comparisons to the zero-error line for training and testing data groups, respectively. Table 5 and Fig. 2a and b provide a testament to the new model's accuracy for both data groups as the model scored low error, mean value slightly higher than the optimal value and coefficient of determination slightly lower than the optimal value.

$$V_{frc} = -3487.502d/(\frac{L_f}{D_f})^3(\frac{a}{d})^3 + 72967859.62\rho_1^2/(\frac{L_f}{D_f})^2(\frac{a}{d})^{1.5} - 202.1093\rho_1^{0.5}/(\frac{L_f}{D_f})^{0.5} + 365.6352\rho_1^{0.5}/d^{0.5} - 665137.294\rho_1^2/d(\frac{a}{d})^{1.5} + 0.0020068V_f^{0.5}d^{1.5} + 0.12937V_fF_c^2/\rho_1^2d^{1.5}(\frac{a}{d})^2 - 164655.6281V_f^3/(\frac{a}{d})^2 + 0.5481 \quad (6)$$

Assessment of the available equations

A statistical assessment is carried out in this section to check the predictions accuracy of available equations, where the MAE, RMSE, μ, and R^2 were calculated for the available equations and compared with the values obtained for the new model (presented in Table 5). Notably, the data

Table 5 Statistical assessment of the proposed model using training and testing data

No	Equation	MAE(kN)	RMSE(kN)	μ	R^2
1	Training data	0.55	0.75	1.05	0.93
2	Testing data	0.63	0.82	1.05	0.93

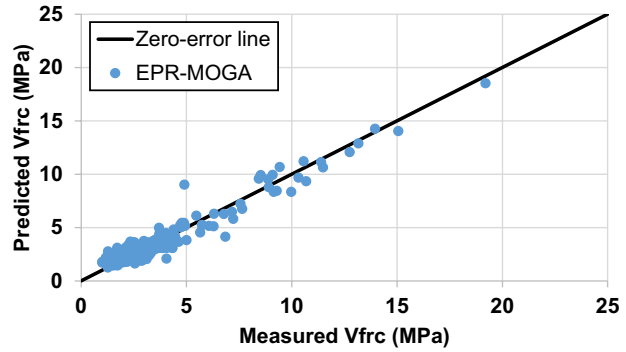

a) Training data

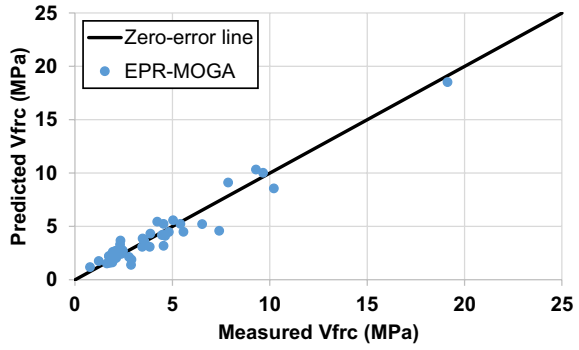

b) Testing data

Fig. 2 Relationship between predictions of the new model and the measured values of *Vfrc* for: **a** training group; **b** testing group

Table 6 Statistical assessment of the available equations using training data

No	Equation	MAE	RMSE	Mean	R^2
1	Al-Ta'an and Al-Fee [5]	1.77	4.14	1.06	0.37
2	Ashour et al. [17]	1.88	3.20	1.20	0.36
3	Gandomi et al. [20]	1.28	1.93	1.26	0.58
4	Kara [23]	1.97	3.46	0.90	0.01
5	Khaloo and Kim [25]	1.90	2.65	1.45	0.16
6	Khuntia et al. [26]	1.93	3.02	0.78	0.16
7	Kwak et al. [27]	1.62	2.92	1.06	0.42
8	Mansur et al. [29]	2.04	3.32	0.79	0.04
9	Narayanan and Darwish [30]	1.86	3.80	1.01	0.35
10	Swamy and Al-Taan [38]	2.21	3.48	0.72	0.01
11	Sharifi and Moghbeli [35]	0.81	1.03	1.10	0.87
12	Tarawneh et al. [39]	4.07	6.84	2.03	0.08

Table 7 Statistical assessment of the available equations using testing data

No	Equation	MAE	RMSE	Mean	R^2
1	Al-Ta'an and Al-Fee [5]	1.82	3.22	1.05	0.31
2	Ashour et al. [17]	1.96	3.10	1.00	0.28
3	Gandomi et al. [20]	1.54	2.48	1.13	0.38
4	Kara [23]	2.04	3.70	1.21	0.01
5	Khaloo and Kim [25]	1.97	2.95	0.89	0.16
6	Khuntia et al. [26]	2.09	3.38	1.51	0.15
7	Kwak et al. [27]	1.77	2.83	0.75	0.33
8	Mansur et al. [29]	2.20	3.65	0.73	0.04
9	Narayanan and Darwish [30]	1.99	3.27	0.98	0.28
10	Swamy and Al-Taan [29]	2.37	3.79	0.92	0.02
11	Sharifi and Moghbeli [35]	0.90	1.08	1.71	0.89
12	Tarawneh et al. [39]	3.65	6.66	0.69	0.09

groups developed in "EPR-MOGA new model" Section (training and testing) are also utilized here to provide clear comparisons of the accuracy with the new model.

Tables 6 and 7 present the results of the accuracy assessment of these equations for both training and testing data groups. In addition, Figs. 3 and 4 compare the existing

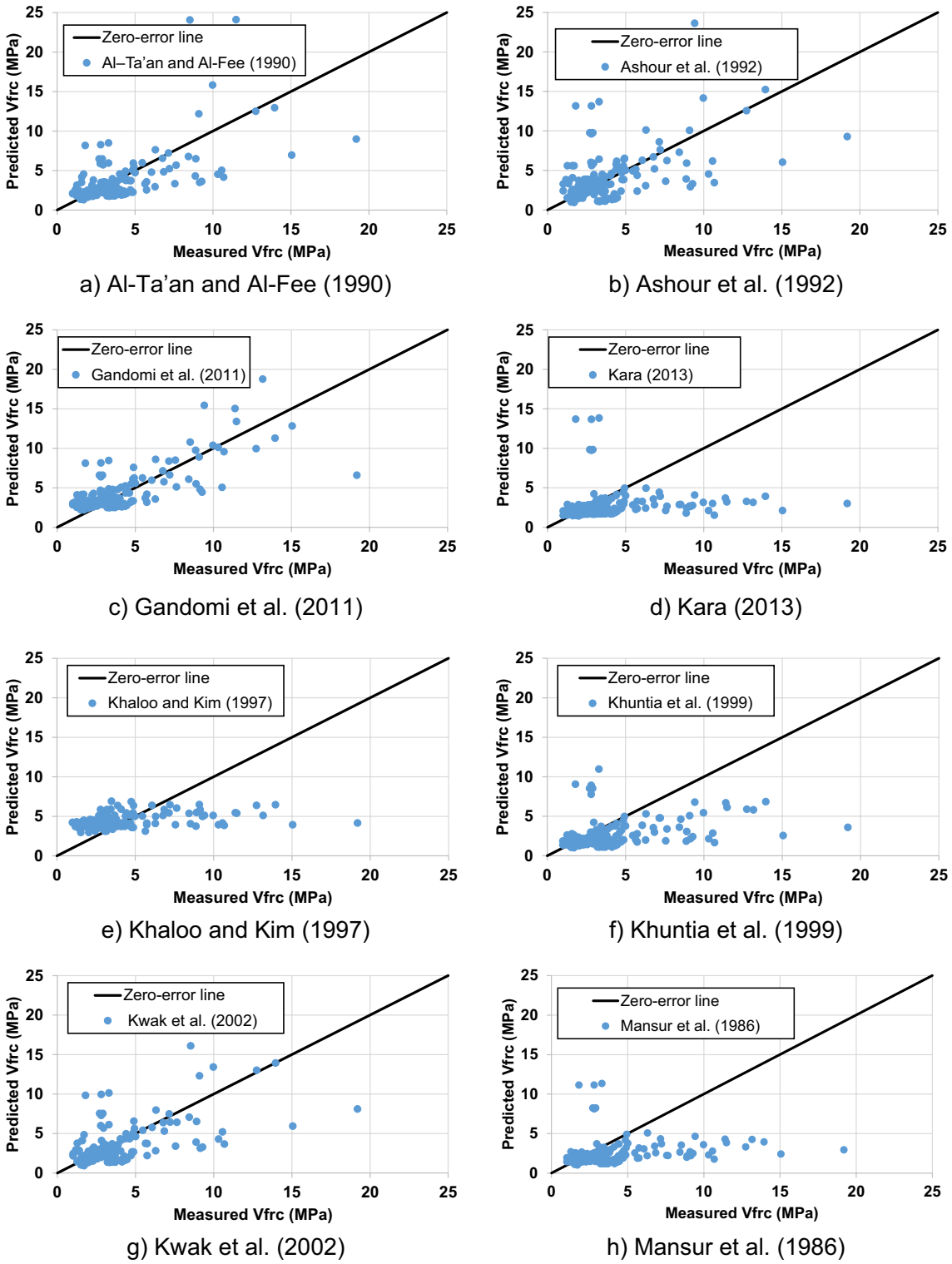

Fig. 3 Relationship between measured and the predicted *V*frc using the available equations for the training data group

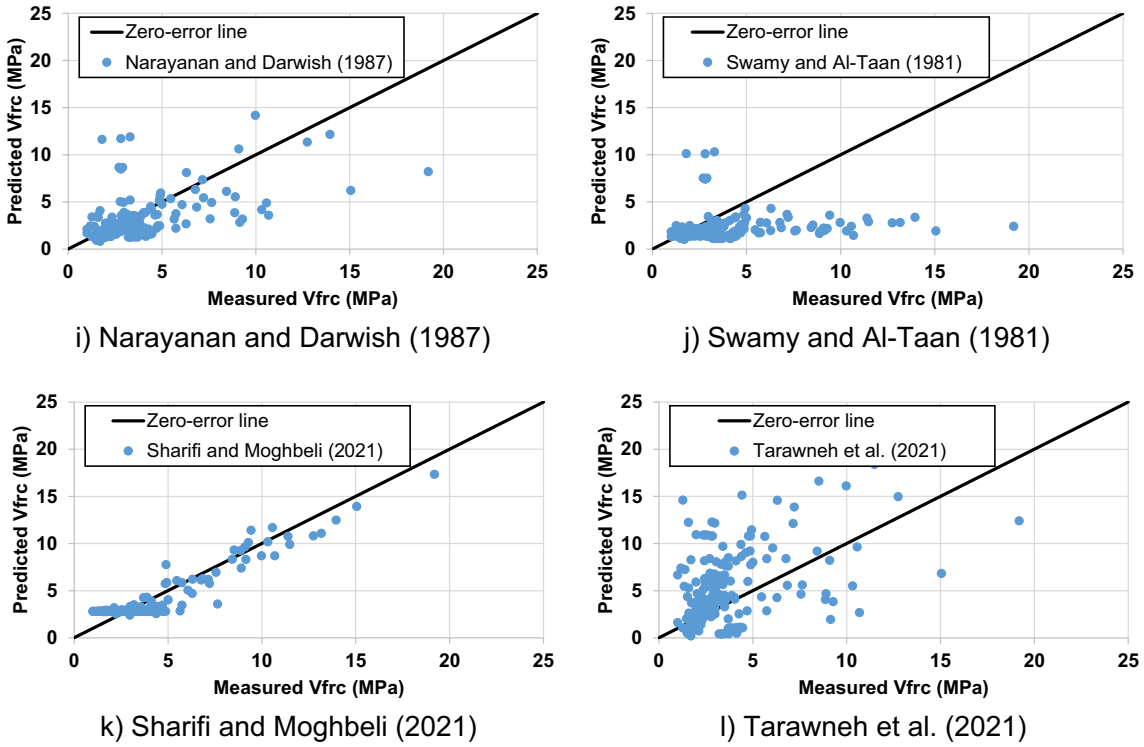

Fig. 3 (continued)

equations' predictions against the zero-error line. It is clear from the tables that the available equations scored an error higher than the new model (i.e., higher values of MAE and RMSE). In addition, the scored values of the R^2 of the available equations are lower than that scored by the new model. Figures 3 and 4 also show that the predictions of the available equations have significant scatter compared to the zero-error line, while the new model showed less scatter (Fig. 2a, b). Thus, it could be stated that the new model provides better accuracy than the available equations. Importantly, it should be noted that the equation of Sharifi and Moghbeli [35] scored lower MAE and RMSE, and higher R^2 compared to other available equations for both data groups.

Error analysis

Finally, an error analysis is carried out to compare the accuracy of the new EPR-MOGA model with the available equations in the literature. This was done by obtaining and plotting the relationship between the cumulative frequency and error level using the methodology employed by many previous studies (e.g., [11, 15, 33]. The results are presented in Fig. 5 for the new model (denoted as EPR-MOGA) and the available equations. It is evident from the figure that the new model scored significantly better than the available equations as it achieved higher frequency with lower error compared to the available equations. For instance, the new model scored 70% cumulative frequency at an error level of 20%, while the available equations scored cumulative frequency between 16 and 53%. It is also clear from Fig. 5 that the equation of Sharifi and Moghbeli [35] scored second, and thus, it could be considered as the best available equation. Lastly, the equation developed by Tarawneh et al. [39] provided the worst cumulative frequency of error for error range of 20–59%.

In conclusion, it is evident based on the assessment presented in Sections "EPR-MOGA new model" "Assessment of the available equations" and "Error analysis" that the new model is superior and outperformed the available equations. Thus, the new model could be used to reduce uncertainty and increase the accuracy in the calculation of the shear capacity.

Conclusions

Using data collected from the literature, this study used the cutting-edge EPR-MOGA technique to develop new equation to predict the shear capacity of steel fibre reinforced concrete (SFRC) beams. The outcomes demonstrated that the new strategy led to significantly higher accuracy. Therefore, the results of this work offer a potentially powerful and straightforward approach for designers and have shown

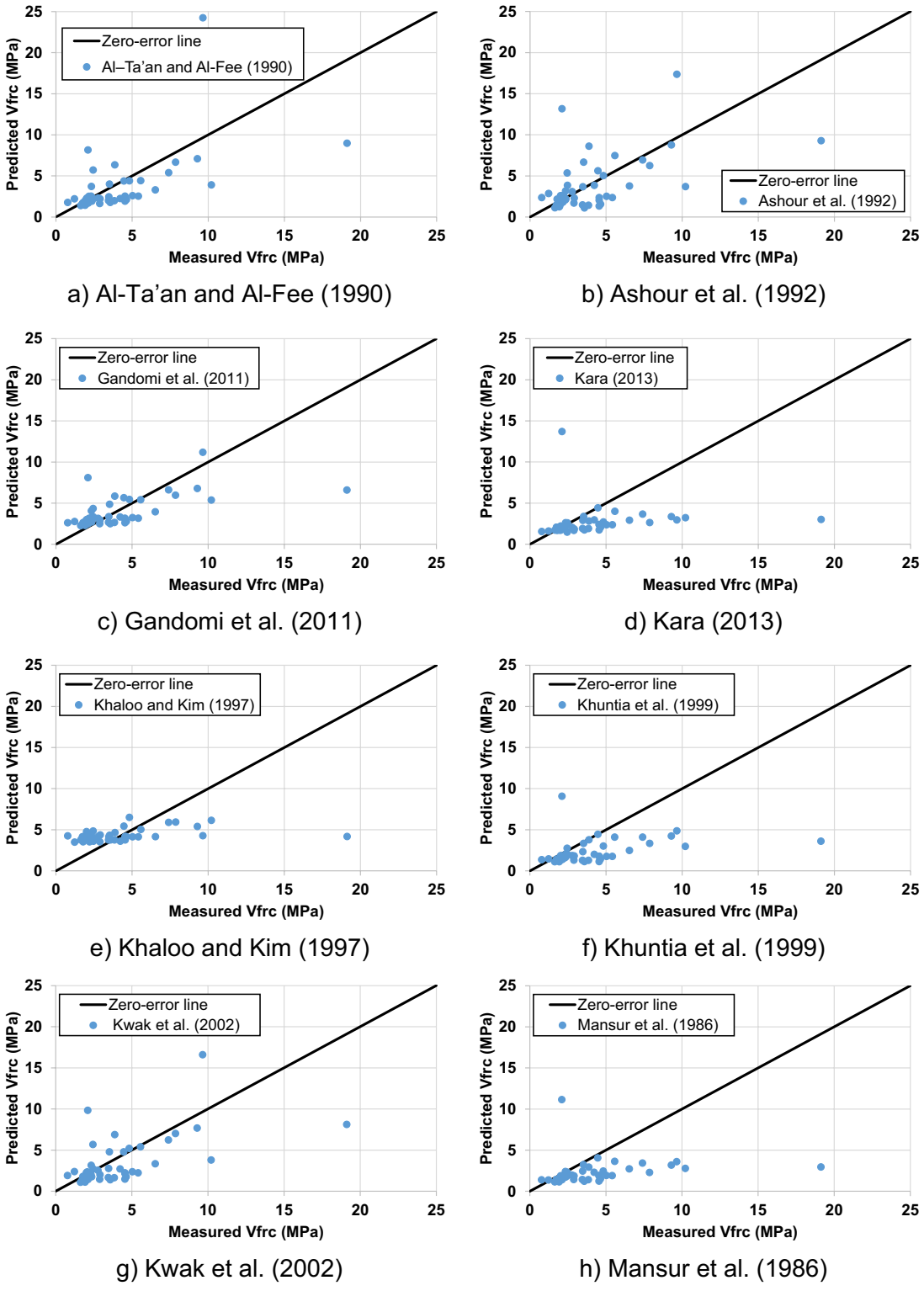

Fig. 4 Relationship between measured and the predicted $Vfrc$ using the available equations for the testing data group

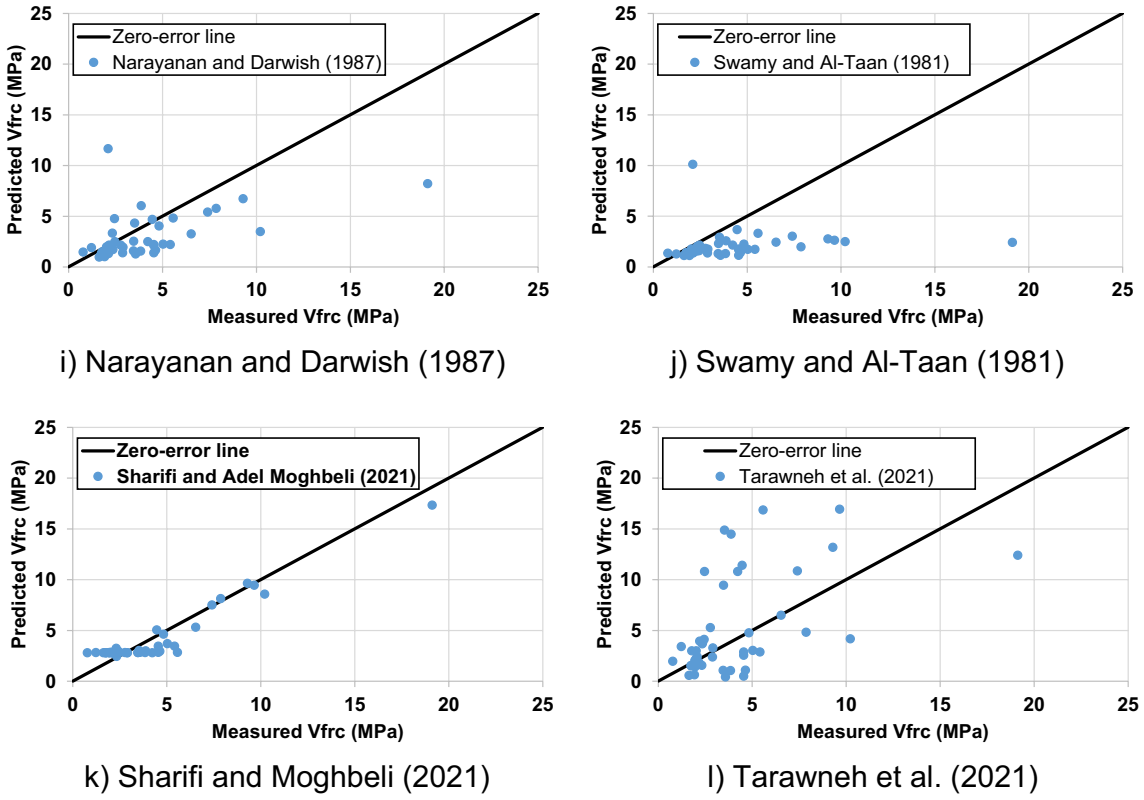

Fig. 4 (continued)

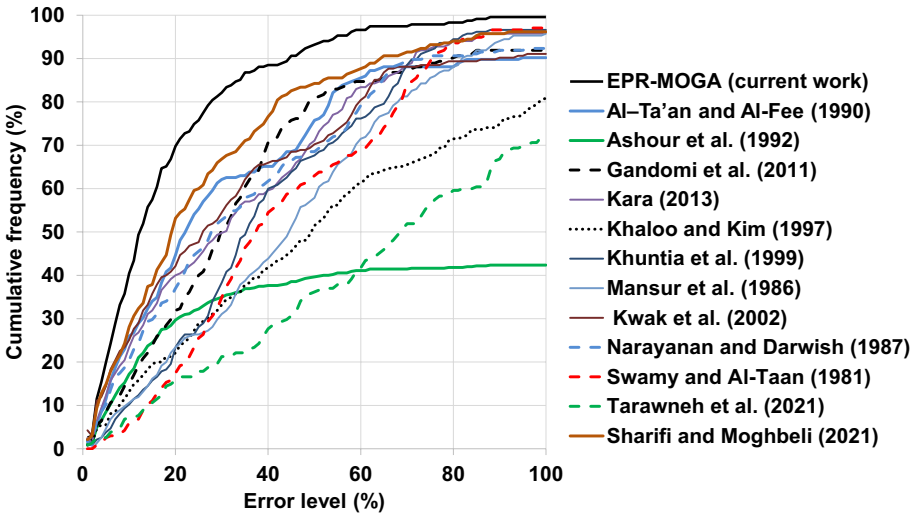

Fig. 5 Results of the cumulative frequency and error level relationship for the new model and the available equations

enhanced accuracy compared to previous equations available in the literature to predict shear capacity of SFRC beams. The following conclusions can be formed, taking into account the limitations of the work presented:

1 The proposed equation showed accuracy better than the available equations in the literature, with R^2 equal to 0.93 for the training set and 0.93 for the testing set compared to the equations available in the literature where these equations scored R^2 between 0.01 and 0.89. In addition, the new model also scored lower error (i.e., lower MAE and RMSE) compared to the available equations.
2 The current model achieved better performance as it has been developed using this database and therefore, the

3 The best equation available in the literature to predict the shear capacity of SFRC beams is the equation proposed by Sharifi and Moghbeli [35], where it recorded R^2 equal to 0.87 for the training set and 0.89 for the testing set. This equation also scored better than the other available equations in terms of the cumulative frequency of error.
4 Based on the cumulative frequency of error, it could be stated that the equation of Tarawneh et al. [39] provides the poorest predictions for error level range of 20–59%.

Finally, it is important to state that one of the reasons that the model developed in this research achieved better performance than the other empirical equations is because this model has been developed using the same database which has been used to examine the accuracy performance, while the other empirical equations have been developed using other limited datasets. However, it is significant to stress that our work has demonstrated a rational methodology for putting into practice a soft computing strategy employing an AI algorithm to create novel robust model that could be used with confidence to predict the shear capacity of steel fibre reinforced concrete (SFRC) beams.

Declarations

Conflict of interest Authors have no conflict of interest to declare.

Ethical approval The authors state that the research was conducted according to ethical standards.

Open Access This article is licensed under a Creative Commons Attribution 4.0 International License, which permits use, sharing, adaptation, distribution and reproduction in any medium or format, as long as you give appropriate credit to the original author(s) and the source, provide a link to the Creative Commons licence, and indicate if changes were made. The images or other third party material in this article are included in the article's Creative Commons licence, unless indicated otherwise in a credit line to the material. If material is not included in the article's Creative Commons licence and your intended use is not permitted by statutory regulation or exceeds the permitted use, you will need to obtain permission directly from the copyright holder. To view a copy of this licence, visit http://creativecommons.org/licenses/by/4.0/.

References

1. ACI Committee 318 (2011) Building code requirements for structural concrete (ACI 318M–11) and commentary (ACI 318R–11). American Concrete Institute, Farmington
2. ACI Committee 445 (1998) Recent approaches to shear design of structural concrete. J Struct Eng 1374–417.https://doi.org/10.1061/(ASCE)0733-9445(1998)124:12(1375).
3. Ahangar-Asr A, Faramarzi A, Mottaghifard N, Javadi AA (2011) Modeling of permeability and compaction characteristics of soils using evolutionary polynomial regression. Comput Geosci 37(11):1860–1869
4. Alani AM, Faramarzi A (2014) An evolutionary approach to modelling concrete degradation due to sulphuric acid attack. Appl Soft Comput 24:985–993
5. Al-Ta'an SA, Al-Feel JR (1990) Evaluation of shear strength of fibre-reinforced concrete beams. Cement Concr Compos 12(2):87–94
6. Al-Hamd R, Gillie M, Warren H, Torelli G, Stratford T, Wang Y (2018) The effect of load-induced thermal strain on flat slab behaviour at elevated temperatures. Fire Saf J 97:12–18. https://doi.org/10.1016/j.firesaf.2018.02.004
7. Al-Hamd R, Gillie M, Cunningham LS, Warren H, Albostami AS (2019) Novel shearhead reinforcement for slab-column connections subject to eccentric load and fire. Arch Civil Mech Eng 19:503–524
8. Alzabeebee S, Chapman DN (2020) Evolutionary computing to determine the skin friction capacity of piles embedded in clay and evaluation of the available analytical methods. Trans Geotech 24:100372
9. Alzabeebee S (2019) Seismic response and design of buried concrete pipes subjected to soil loads. Tunn Undergr Space Technol 93:103084
10. Alzabeebee S (2022) Application of EPR-MOGA in computing the liquefaction-induced settlement of a building subjected to seismic shake. Eng Comput 38:437–448. https://doi.org/10.1007/s00366-020-01159-9
11. Alzabeebee S (2022) Explicit soft computing model to predict the undrained bearing capacity of footing resting on aggregate pier reinforced cohesive ground. Innov Infrastruct Solut 7(1):1–10
12. Alzabeebee S, Chapman DN, Faramarzi A (2018) Development of a novel model to estimate bedding factors to ensure the economic and robust design of rigid pipes under soil loads. Tunn Undergr Space Technol 71:567–578
13. Alzabeebee S, Chapman DN, Faramarzi A (2019) Economical design of buried concrete pipes subjected to UK standard traffic loading. Proc Inst Civil Eng Struct Build 172(2):141–156
14. Alzabeebee S, Mohamad SA, Al-Hamd RKS (2021) Surrogate models to predict maximum dry unit weight, optimum moisture content and California bearing ratio form grain size distribution curve. Road Mater Pavement Des 23:1–18
15. Alzabeebee S, Mohammed DA, Alshkane YM (2022) Experimental study and soft computing modeling of the unconfined compressive strength of limestone rocks considering dry and saturation conditions. Rock Mech Rock Eng. https://doi.org/10.1007/s00603-022-02948-y
16. Alzabeebee S, Dhahir MK, Keawsawasvong S (2022) Predictive model for the shear strength of concrete beams reinforced with longitudinal FRP bars. Struct Eng Mech 84(2):143–154. https://doi.org/10.12989/sem.2022.84.2.000
17. Ashour SA, Hasanain GS, Wafa FF (1992) Shear behavior of high-strength fiber reinforced concrete beams. Struct J 89(2):176–184
18. Batson G, Jenkins E, Spatney R (1972) Steel fibers as shear reinforcement in beams. ACI J Proc 69(10):640–644
19. Bui TT, Nana WSA, Doucet-Ferru B, Bennani A, Lequay H, Limam A (2020) Shear performance of steel fiber reinforced concrete beams without stirrups: experimental investigation. Int J Civil Eng 18(8):865–881
20. Gandomi AH, Alavi AH, Yun GJ (2011) Nonlinear modeling of shear strength of SFRC beams using linear genetic programming. Struct Eng Mech 38(1):1–25
21. Giustolisi O, Savic DA (2009) Advances in data-driven analyses and modelling using EPR-MOGA. J Hydroinf 11(3–4):225–236
22. Javadi AA, Ahangar-Asr A, Johari A, Faramarzi A, Toll D (2012) Modelling stress–strain and volume change behaviour of unsaturated soils using an evolutionary based data mining technique, an incremental approach. Eng Appl Artif Intell 25(5):926–933

23. Kara IF (2013) Empirical modeling of shear strength of steel fibre reinforced concrete beams by gene expression programming. Neural Comput Appl 23(3):823–834
24. Karl KW, Kim KS, Lee DH (2010) An experimental study on shear strength of high-strength reinforced concrete beams with steel fibers. J Archit Inst Korea 27(10):19–28
25. Khaloo AR, Kim N (1997) Influence of concrete and fibre characteristics on behavior of steel fibre reinforced concrete under direct shear. Mater J 94(6):592–601
26. Khuntia M, Stojadinovic B, Goel SC (1999) Shear strength of normal and high-strength fibre reinforced concrete beams without stirrups. Struct J 96(2):282–289
27. Kwak YK, Eberhard MO, Kim WS, Kim J (2002) Shear strength of steel fibre-reinforced concrete beams without stirrups. ACI Struct J 99(4):530–538
28. Lim TY, Paramasivam P, Lee SL (1987) Shear and moment capacity of reinforced steel-fibre-concrete beams. Mag Concr Res 39(140):148–160
29. Mansur MA, Ong KCG, Paramasivam P (1986) Shear strength of fibrous concrete beams without stirrups. J Struct Eng 112(9):2066–2079
30. Narayanan R, Darwish IYS (1987) Use of steel fibers as shear reinforcement. ACI Struct J 84(3):216–227
31. Nassr A, Javadi A, Faramarzi A (2018) Developing constitutive models from EPR-based self-learning finite element analysis. Int J Numer Anal Meth Geomech 42(3):401–417
32. Oh YH, Kim JH (2008) Estimation of flexural and shear strength for steel fiber reinforced flexural members without shear reinforcements. J Korea Concr Inst 20(2):257–267
33. Padmini D, Ilamparuthi K, Sudheer KP (2008) Ultimate bearing capacity prediction of shallow foundations on cohesionless soils using neurofuzzy models. Comput Geotech 35(1):33–46
34. Rezania M, Faramarzi A, Javadi AA (2011) An evolutionary based approach for assessment of earthquake-induced soil liquefaction and lateral displacement. Eng Appl Artif Intell 24(1):142–153
35. Sharifi Y, Moghbeli A (2021) Shear capacity assessment of steel fibre reinforced concrete beams using artificial neural network. Innov Infrastruct Solut 6(2):1–19
36. Swamy RN, Bahia HM (1978) Influence of fibre reinforcement on the dowel resistance to shear. J Am Concr Inst. https://doi.org/10.14359/6950
37. Swamy RN and Bahia HM (1985) Effectiveness of steel fibre as shear reinforcement. Concr. Int. 7.
38. Swamy RN, AI-Taan SA (1981) Deformation and ultimate strength in flexure of reinforced concrete beams made with steel fibre concrete. ACI Struct J 78(5):395–405
39. Tarawneh A, Almasabha G, Alawadi R, Tarawneh M (2021) Innovative and reliable model for shear strength of steel fibres reinforced concrete beams. Structures 32:1015–1025
40. Zsutty TC (1968) Beam shear strength prediction by analysis of existing data. ACI Struct J 65(11):943–951
41. Zuhaira AA, Al-Hamd RKS, Alzabeebee S, Cunningham LS (2021) Numerical investigation of skimming flow characteristics over non-uniform gabion-stepped spillways. Innov Infrastruct Solut 6(4):1–19
42. Wu C, Hong L, Wang L, Zhang R, Pijush S, Zhang W (2022) Prediction of wall deflection induced by braced excavation in spatially variable soils via convolutional neural network. Gondwana Res. https://doi.org/10.1016/j.gr.2022.06.011
43. Zhang W, Wu C, Zhong H, Li Y, Wang L (2021) Prediction of undrained shear strength using extreme gradient boosting and random forest based on Bayesian optimization. Geosci Front 12(1):469–477
44. Zhang W, Wu C, Li Y, Wang L, Samui P (2021) Assessment of pile drivability using random forest regression and multivariate adaptive regression splines. Georisk Assess Manag Risk Eng Syst Geohazards 15(1):27–40